slight shift of the visible band in spectrum E' of Figure 7 suggest the existence of the pulsed state.[35,36] The slow decay rate constant that we observe is consistent with the pulsed to resting transition reported by others[35] so we tentatively make that assignment. The overall decay of II_m under our conditions may, therefore, be written as

$$II_m \underset{k_{on} = 7 \times 10^2\ M^{-1}\ s^{-1}}{\overset{k_{off} = 5 \times 10^{-3}\ s^{-1}}{\rightleftharpoons}} H_2O_2 + \text{pulsed} \xrightarrow{k = 5 \times 10^{-4}\ s^{-1}} \text{resting}$$

Additional experiments are needed to confirm this decay mechanism.

Acknowledgment. S.H. was partially supported by Grant GM-39359 from the National Institute of General Medical Sciences. We thank Dr. G. Blondin of Water Resources Center for mitochondria.

Registry No. O_2, 7782-44-7; cytochrome *c* oxidase, 9001-16-5.

(35) Kumar, C.; Naqui, A.; Chance, B. *J. Biol. Chem.* **1984**, *259*, 11668-11671.
(36) Brunori, M.; Colosimo, A.; Rainoni, G.; Wilson, M. T.; Antonini, E. *J. Biol. Chem.* **1979**, *254*, 10769-10775.
(37) Hill, B. C.; Greenwood, C. *Biochem. J.* **1984**, *218*, 913-921.
(38) Orii, Y. *J. Biol. Chem.* **1984**, *259*, 7187-7190.

Single-Crystal Electron Spin-Echo Envelope Modulation Study of Cu(II)-Doped Zinc Bis(1,2-dimethylimidazole) Dichloride

Michael J. Colaneri,*,† Joseph A. Potenza,‡ Harvey J. Schugar,‡ and Jack Peisach†

Contribution from the Department of Molecular Pharmacology, Albert Einstein College of Medicine of Yeshiva University, 1300 Morris Park Avenue, Bronx, New York 10461, and Department of Chemistry, Rutgers, The State University of New Jersey, New Brunswick, New Jersey 08903. *Received March 12, 1990*

Abstract: Single crystals of copper-doped zinc bis(1,2-dimethylimidazole) dichloride were studied with electron spin-echo envelope modulation (ESEEM) spectroscopy. Modulation frequencies apparent through Fourier transformation of the ESEEM decay curves were attributed to interactions between the Cu(II) unpaired electron and remote ^{14}N nuclei of the two coordinated dimethylimidazole ligands. Hyperfine and quadrupole coupling tensors were fit to the observed magnetic field angular dependencies of these frequencies according to a least-squares criterion. The two remote nitrogen atoms, although formally magnetically distinct, give essentially equivalent coupling tensor principal values. This agrees with the noncrystallographic, 2-fold rotation relationship between the two dimethylimidazole rings around the metal ion in the host crystal structure. The isotropic part of the ^{14}N hyperfine tensor was found to be smaller than reported in other model imidazole compounds previously studied by ESEEM spectroscopy in frozen solutions. This trend is consistent with the change in geometry of ligands around the copper from presumed approximate square planar in frozen solution to near tetrahedral in the present system. The maximum hyperfine principal direction is not along the Cu(II)-N(remote) vector but subtends an angle of ≈40° from this direction. A simple multipoint electron spin-nucleus dipolar hyperfine calculation failed to reconcile this difference. This result and others suggest that a nonnegligible contribution to the hyperfine coupling originates from spin density located on the imidazole ring. The quadrupole tensor principal directions, on the other hand, correlate with the local geometry about the remote nitrogen. In addition, the quadrupole principal values were found to be similar to those reported previously for solid *N*-benzylimidazole.

I. Introduction

X-ray crystallographic analysis of numerous blue copper proteins[1] show metal ion geometries that deviate greatly from the normally found distorted octahedral ligand arrangement around copper in model compounds. These copper sites known as type 1[2] have geometries best described as elongated C_{3v} whose equatorial coordination consists of two histidinyl imidazole nitrogens and a cysteinyl sulfur in an approximate trigonal plane; the Cu(II) is displaced toward a distant apical methionyl sulfur to complete the arrangement.[1] In view of this biological prevalence for low-symmetry copper sites it was of our interest to study the magnetic parameters of remotely coupled nitrogens in copper models having geometries that differ from the most commonly found near-square-planar coordination.[3] We have therefore initiated a systematic single-crystal electron spin-echo envelope modulation (ESEEM) analysis of remote nitrogen couplings to copper in known geometrical sites in the hope that accurate hyperfine and quadrupole tensors may aid similar studies of copper models and metalloproteins.

The present report deals with copper doped into single crystals of Zn(II)(1,2-dimethylimidazole)$_2$Cl$_2$. X-ray diffraction analysis has shown the zinc complex to exhibit a distorted tetrahedral geometry.[4,5] Although previous ESEEM studies have been performed on imidazole models bound to copper in frozen solutions,[6-8] the analysis of an imidazole compound in a tetrahedral

† Albert Einstein College of Yeshiva University.
‡ Rutgers, The State University of New Jersey.

(1) (a) Adman, E. T.; Turley, S.; Bramson, R.; Petratos, K.; Banner, D.; Tsernoglou, D.; Beppu, T.; Watanabe, H. *J. Biol. Chem.* **1989**, *264*, 87. (b) Guss, J. M.; Merritt, E. A.; Phizackerley, R. P.; Hedman, B.; Murata, M.; Hodgson, K. O.; Freeman, H. C. *Science* **1988**, *241*, 806. (c) Korszun, Z. R. *J. Mol. Biol.* **1987**, *196*, 413. (d) Adman, E. T.; Stenkamp, R. E.; Sieker, L. C.; Jensen, L. H. *J. Mol. Biol.* **1978**, *123*, 35. (e) Adman, E. T.; Jensen, L. H. *Isr. J. Chem.* **1981**, *21*, 8. (f) Colman, P. M.; Freeman, H. C.; Guss, J. M.; Murata, M.; Norris, V. A.; Ramshaw, J. A. M.; Venkatappa, M. P. *Nature* **1978**, *272*, 319. (g) Guss, J. M.; Freeman, H. C. *J. Mol. Biol.* **1983**, *169*, 521. (h) Church, W. B.; Guss, J. M.; Potter, J. J.; Freeman, H. C. *J. Biol. Chem.* **1986**, *261*, 234. (i) Norris, G. E.; Anderson, B. F.; Baker, E. N.; Rumball, S. V. *J. Mol. Biol.* **1979**, *135*, 309. (j) Norris, G. E.; Anderson, B. F.; Baker, E. N. *J. Mol. Biol.* **1983**, *165*, 501. (k) Norris, G. E.; Anderson, B. F.; Baker, E. N. *J. Am. Chem. Soc.* **1986**, *108*, 2784. (l) Baker, E. N. *J. Mol. Biol.* **1988**, *203*, 1071.
(2) Malkin, R.; Malmström, B. G. *Adv. Enzymol.* **1970**, *33*, 177.
(3) (a) Orgel, L. E. *An Introduction to Transition-Metal Chemistry: Ligand-Field Theory*; John Wiley and Sons: New York, 1960; pp 57-60. (b) Hathaway, B. J. In *Comprehensive Coordination Chemistry*; Wilkinson, G., Ed.; Pergamon Press: New York, 1987; pp 594-744.
(4) Bharadwaj, P.; Potenza, J.; Schugar, H. J., unpublished work.
(5) The angle between the N-Zn-N and Cl-Zn-Cl planes is ≈88°.
(6) Mims, W. B.; Peisach, J. *J. Chem. Phys.* **1978**, *69*, 4921.

0002-7863/90/1512-9451$02.50/0

geometry around copper had not been attempted. Previously determined electron paramagnetic resonance (EPR) parameters on this copper-doped crystal system resembled those found in type I copper sites.[9] Optical measurements and theoretical self-consistent-field–Xα–scattered wave (SCF–Xα–SW) combined with ligand-field calculations were carried out to provide a detailed description of the unpaired electron wave function over the copper coordinated ligand atoms.[9] Similar features in the electron spin orbital were found in comparable calculations of the blue copper sites.[9] The present single-crystal system is therefore of particular interest for ESEEM study for the following reasons. First, accurate remote nitrogen hyperfine and quadrupole tensors for an imidazole model compound in a tetrahedral environment about copper may be representative of similar interactions of the remote nitrogens of the coordinated histidines in type I copper sites. Second, the detailed analysis of the singly occupied copper orbital provides an assessment of whether a simple multipoint electron spin model can correctly predict the hyperfine tensor anisotropies of the two remote ^{14}N nuclei. Finally, an analysis can be made concerning the complexity involving an ESEEM determination of accurate tensors for two similarly coupled nitrogens near the "cancellation" region[6,10] where multinuclear combination frequencies[11,12] are anticipated.

II. Experimental Section

Zinc chloride (99.999%), copper(II) chloride (99.999%), and 1,2-dimethylimidazole were obtained from Aldrich Chemicals. 1,2-Dimethylimidazole was further purified by vacuum distillation. Pale-orange crystals shaped as rectangular plates with longest dimension 2–3 mm along the b axis grew from slow evaporation of an acetone solution of $ZnCl_2$ and 1,2-dimethylimidazole in 1:2 mole ratio, containing 1–5 mol % $CuCl_2$. The estimated copper doping was considerably lower than its solution concentration. Crystals were affixed with vacuum grease (Dow Corning) to the wall of an X-band TE_{110} rectangular reflection cavity described by Mims[13] and subsequently quenched to liquid helium temperature by immersion into the electron spin echo (ESE) spectrometer dewar.[7] The cavity rotatable side wall was kept fixed and crystals were respectively mounted with their b, c, and $a' = b \times c$ axes parallel to magnetic field rotation for data collection. Crystal mounting uncertainties were ± 3° as estimated from repetitive measurements. The Zn(II)(1,2-dimethylimidazole)$_2Cl_2$ complex crystallizes in space group $P2_1/c$ with one molecule of the complex comprising the asymmetric unit.[9] Further analysis shows that the two dimethylimidazole ligands are related by a noncrystallographic 2-fold rotation axis. Previous EPR measurements support the assumption that the copper dopant conforms to the crystalline environment of the zinc host.[9] Echo envelope decay curves were typically acquired at 5° intervals of the magnetic field orientation.

An ESE spectrometer described previously was utilized for the generation of electron spin–echoes and detection of the stimulated (three-pulse) echo envelope decay.[7] The pulse sequence $\pi/2$–τ–$\pi/2$–T–$\pi/2$–τ(echo) was utilized with the first two $\pi/2$ pulses 180° phase shifted on alternate sequences to eliminate detection of an unwanted secondary echo. Although the cavity Q was variable from ≈200 to 1000, its minimal value setting was essential when the 20-ns microwave pulses were used to reduce cavity ringing artifacts. Nevertheless, τ, the time delay between first and second microwave pulse could usually not be made lower than 350 ns. The resonant frequency could be adjusted (≈9–10 GHz) by the relative location of a Teflon plunger inside the cavity, and this flexibility aided the assignments of some of the modulation frequencies as discussed below. The echo envelope decay patterns were measured for time $\tau + T$ where τ remains constant and T, the time between the second and third microwave pulse, varied from 0.08 to 40.04 μs. A data set consisted of 1024 points, with the last 25 sampling the baseline. Every data point was averaged 10–20 times during a single ESE envelope decay scan. A 10-Hz repetition of the three-pulse sequence and microwave pulse power of ≈400 W gave maximum echo intensities.

Table I. g Tensor and the Refined Hyperfine and Quadrupole Coupling Tensors for the Two Weakly Interacting Remote Nitrogens in Single Crystals of Cu(II)-Doped Zn(II)(1,2-dimethylimidazole)$_2Cl_2$[a]

	principal values		direction cosines a'	b	c
	g Tensor				
	2.367		0.357	0.065	0.932
	2.148		0.476	0.846	−0.241
	2.049		0.804	−0.529	−0.271
	Hyperfine Tensor				
	MHz	a_{iso}			
N1	1.75		0.9542	−0.2483	−0.1671
	1.28	1.42	0.0321	−0.4701	0.8820
	1.22		0.2976	0.8470	0.4406
N4	1.70		0.8693	−0.1490	−0.4713
	1.24	1.37	0.2917	−0.6152	0.7324
	1.18		0.3991	0.7741	0.4914
	Quadrupole Tensor				
	MHz				
N1	0.62		−0.5780	−0.1454	0.8030
	0.48		−0.3095	0.9495	−0.0509
	−1.10		0.7550	0.2779	0.5939
N4	0.64		0.9524	0.2158	0.2153
	0.50		−0.2701	0.9250	0.2674
	−1.14		−0.1414	−0.3128	0.9392

$\langle e^2qQ \rangle = -2.236$ MHz, $\langle \eta \rangle = 0.127$.

[a] The g tensor and refined nitrogen coupling tensors were determined according to methods described in the text.

Time-domain data were extrapolated to $\tau + T = 0$ by using eq 3 in ref 14 and subsequently Fourier transformed and plotted as reported previously.[7] The measured ^{14}N modulation frequencies thus obtained were followed as a function of magnetic field orientation in the three orthogonal planes. These data were used to least-squares fit ^{14}N coupling parameters to a spin Hamiltonian

$$\mathcal{H} = \beta S \cdot g \cdot H + I \cdot A \cdot S - g_n \beta_n H \cdot I + I \cdot Q \cdot I \qquad (1)$$

for each nitrogen by methods described earlier by Castellano and Bothner-By.[15] Adjustable parameters included the six hyperfine (A) components and five independent elements of the traceless quadrupole tensor (Q). Other terms in the above equation have been explained elsewhere.[16] Least-squares calculations were performed using a modified version of a program previously written for the analysis of bromine ENDOR measurements.[17] The complete g tensor was obtained from data in Figure 10 of ref 9[18] and is listed in Table I. ESEEM simulations at discrete magnetic field orientations were accomplished with computer software incorporating a small section of existing code for powder ESEEM simulations written by Dr. J. Cornelius.[19] Similar to the approach used by Reijerse et al.,[20] the equations derived by Mims[21] were utilized to also take into account mixing of the electronic spin states by the ^{14}N couplings. All ESEEM simulations were multiplied by a decay function $\exp((-0.7\pi(T + \tau)/40\ \mu s)^{3/2})$, where $T + \tau$ is in microseconds. Fourier transformation (FT) and plotting of the FT-ESEEM simulations were performed with an existing program.[19] In addition to least-squares analysis and simulations, other various calculations described below utilized a MicroVax II computer.

III. Results and Discussion

Determination of the ^{14}N Coupling Parameters. A typical ESEEM decay curve is illustrated in Figure 1. The spectrometer effective dead time, $\tau + T \approx 430$ ns, comprised only a small percentage of the total data set and therefore, except for the

(7) McCracken, J.; Peisach, J.; Dooley, D. M. *J. Am. Chem. Soc.* **1987**, *109*, 4064.
(8) McCracken, J.; Pember, S.; Benkovic, S. J.; Villafranca, J. J.; Miller, R. J.; Peisach, J. *J. Am. Chem. Soc.* **1988**, *110*, 1069.
(9) Gewirth, A. A.; Cohen, S. L.; Schugar, H. J.; Solomon, E. I. *Inorg. Chem.* **1987**, *26*, 1133.
(10) Flanagan, H. L.; Singel, D. J. *J. Chem. Phys.* **1987**, *87*, 5606.
(11) Mims, W. B. *Phys. Rev.* **1972**, *B5*, 2409.
(12) Dikanov, S. A.; Shubin, A. A.; Parmon, V. N. *J. Magn. Reson.* **1981**, *42*, 474.
(13) Mims, W. B. *Phys. Rev.* **1964**, *133*, A835.
(14) Mims, W. B. *J. Magn. Reson.* **1984**, *59*, 291.
(15) Castellano, S.; Bothner-By, A. A. *J. Chem. Phys.* **1964**, *41*, 3863.
(16) Wertz, J. E.; Bolton, J. R. In *Electron Spin Resonance: Elementary Theory and Practical Applications*; McGraw-Hill, Inc.: New York, 1972.
(17) Colaneri, M. J.; Box, H. C. *J. Chem. Phys.* **1986**, *84*, 1926.
(18) The rotations in Figure 10 of Gewirth et al.[9] are mislabeled. Correct axis assignments in the reference planes are from left to right *bcb* (around *a'*), *ca'c* (around *b*) and *ba'b* (around *c*).
(19) Cornelius, J. B.; McCracken, J.; Clarkson, R. B.; Belford, R. L.; Peisach, J. *J. Phys. Chem.* **1990**, *94*, 6977.
(20) Reijerse, E. J.; Paulissen, M. L. H.; Keijzers, C. P. *J. Magn. Reson.* **1984**, *60*, 66.
(21) Mims, W. B. *Phys. Rev.* **1972**, *B6*, 3543.

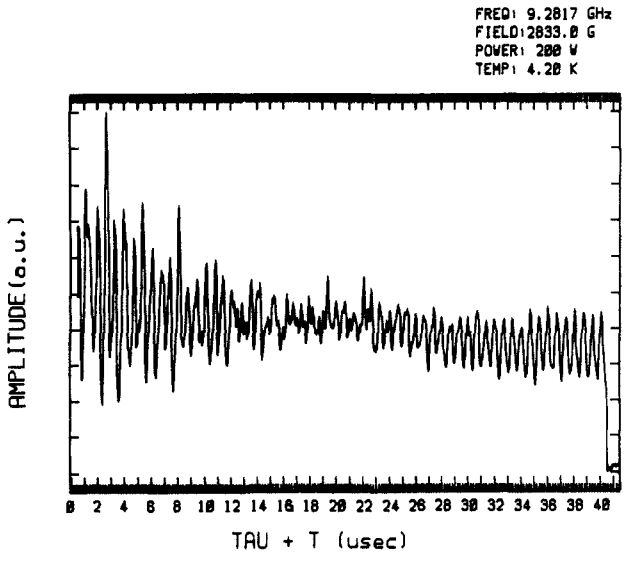

Figure 1. Typical three-pulse electron spin echo envelope time decay spectrum from a single crystal of Cu(II)-doped Zn(II)(1,2-dimethylimidazole)$_2$Cl$_2$ at a specific magnetic field orientation. τ, The time interval between the first two microwave pulses was kept at a constant value of 438 ns, and T, the time between second and third pulse, was allowed to vary.

extrapolation noted above, no further reconstruction was performed. Fourier transformation of similar curves obtained with H aligned along the a', b, and c axes are depicted in Figure 2. It became apparent as the FT-ESEEM angular dependencies were measured that the number of modulation frequency lines exceeded those initially expected if two coupled ^{14}N nuclei are independently considered. In the present system, the existence of multinuclear combination lines[11,12] that arise as a consequence of the product of modulations when more than one nucleus couple was quite probable. Although this presented some initial confusion, reasonable assignments for all the ^{14}N frequency lines were made in the manner briefly outlined below.

Previous ESEEM analysis of copper-bound imidazole model systems in frozen solutions has provided rough spectral features and estimates for the modulation frequencies for remotely coupled ^{14}N nuclei.[6-8] An appropriate scheme for this class of couplings is where one electron spin manifold exhibits near-cancellation of the hyperfine and nuclear Zeeman interactions, leaving the nuclear sublevels to approach the pure nuclear quadrupole condition. Consequently, these sublevel energies become nearly independent of both field strength and orientation. Also, the subsequent modulation frequencies have relatively large amplitudes due to the fulfillment of the necessary condition that the eigenfunction description of sublevels of one-electron manifold is a mixture of the sublevels of the other.[10,22] Since the outermost sublevels of the second manifold, i.e., where the hyperfine and nuclear Zeeman terms add, have approximately equivalent dependence on the quadrupole interaction, their energy differences vary with changing field strength by $2g_n\beta_n\Delta H$. The other two transition frequencies in this manifold complement each other in orientational variability due to their roughly equivalent but opposite dependence on the quadrupole interaction.

With these trends in mind, initial experiments were performed at fixed field orientations but different operating frequencies. The resonant fields were adjusted to maintain constant g settings. Figure 3 shows FT-ESEEM spectra with H, the magnetic field, oriented near a' in the $a'c$ plane. The modulation frequencies at 3.75 and 3.98 MHz in the upper left spectrum increase with field strength by $2g_n\beta_n\Delta H$ and were thus assigned to the double-quantum or "$\Delta m_I = 2$" transition of the Ms manifold for each of the two coupled nitrogens where hyperfine and nuclear Zeeman add. Two other frequencies in Figure 3 also increase with changing field by $\approx g_n\beta_n\Delta H$, one of which was later found to be a combination line. In addition, a combination frequency appearing at 5.29 MHz varies with field strength by $\approx 2g_n\beta_n\Delta H$. Angular dependencies of the FT spectra revealed two pairs of smaller frequencies that sum to each of these $\Delta m_I = 2$ frequencies and were thus ascribed to the other energy differences of this manifold. The relatively intense and isotropic pairs of lines at 1.5 and 1.9 MHz were assigned to frequencies in the "pure" quadrupole manifold for the two nitrogens, the higher of these sets of lines connecting the outermost levels. A third set of lines near 0.3 MHz completed the line assignments.

The angular dependencies of these modulation frequencies are illustrated in Figure 4. A series of trial refinements was necessary both to distinguish between closely spaced lines and to correlate the sets of manifold frequencies to the specific ^{14}N interaction. The frequency lines were further assigned on the basis of assumptions that the isotropic hyperfine component is positive and the largest quadrupole coupling is negative. Justification for a negative maximal quadrupole interaction for the remote imidazole nitrogen is given below. Refinements carried out with alternate line assignments were found to only change the signs of the tensor principal values. FT-ESEEM simulations failed to reveal any differences in modulation frequencies or intensities as the hyperfine and quadrupole coupling signs were changed. The sign of the hyperfine interaction thus remains ambiguous.[23]

FT-ESEEM simulations using parameters from trial refinements were performed at discrete field orientations to guide the assignments of some of the frequencies to their specific ^{14}N nucleus. Frequency lines with uncertain assignments or with low amplitudes were excluded from the refinement calculations. All other measurements were given a weight of 1.0. Data consisted of 658 and 528 points for the N1 and N4 nucleus, respectively. The final refined hyperfine and quadrupole coupling tensors are given in Table I.[24] The root mean square deviations of calculated and experimental frequencies were 0.026 and 0.027 MHz for N1 and N4, respectively. The standard deviations in tensor principal values were in the range 0.003–0.005 MHz as determined by a method essentially described by Nelson.[25] An energy level diagram constructed by using the sets of tensors at a field orientation along the a' reference axis is depicted on the left side in Figure 5. The levels as labeled in this diagram correspond to assignments of the modulation frequencies specified in the calculated FT-ESEEM spectra shown on the right side of the figure. The excellent fit between experimental and theoretical spectra both in frequency values and in amplitudes gives added confidence to our line assignments and the obtained tensor parameters. FT-ESEEM simulations using these tensors are also included, beside experimental spectra, in Figures 2 and 3.

Isotropic Hyperfine Coupling. As discussed below, the quadrupole tensor principal directions can be correlated with the local molecular structure of the dimethylimidazole moiety. This correspondence provides a unique assignment of the hyperfine tensors to each of the two coupled nitrogens. The first and second hyperfine tensors listed in Table I are thuse respectively correlated with the two remote nitrogens designated in the zinc crystal structure as N1 and N4.

(22) Mims, W. B.; Peisach, J.; Davis, J. L. *J. Chem. Phys.* **1977**, *66*, 5536.

(23) One should note that in a previous single-crystal ESEEM study of the A(Ti-Li) center in α-quartz (Isoya, J.; Bowman, M. K.; Norris, J. R.; Weil, J. A. *J. Chem. Phys.* **1983**, *78*, 1735) it was possible to experimentally determine the relative signs of the ^{7}Li hyperfine and quadrupole coupling interactions from an analysis of modulation frequency intensity dependencies on the individual EPR transitions, which were resolved in a 2-D ESEEM experiment.

(24) At the request of a reviewer, the affect of g anisotropy on the nitrogen hyperfine tensor was considered and showed that the pseudocontact terms are <0.03 MHz, the spin-only hyperfine A_{max} directions change by <2° and the total anisotropies are smaller by ≈0.03 MHz as compared to the hyperfine tensors fit in the spin Hamiltonian. The copper hyperfine interaction was not included in the least-squares analysis. Rough estimates for the maximum shifts in the ^{14}N modulation frequencies due to this interaction determined from the second-order equations given by S. Kita, M. Hashimoto, and M. Iwaizumi (*Inorg. Chem.* **1979**, *18*, 3432) and R. Calvo, S. B. Oseroff, and H. C. Abache, (*J. Chem. Phys.* **1980**, *72*, 760) were approximately equal to one root mean square deviation of the frequency data.

(25) Nelson, W. H. *J. Magn. Reson.* **1980**, *38*, 71.

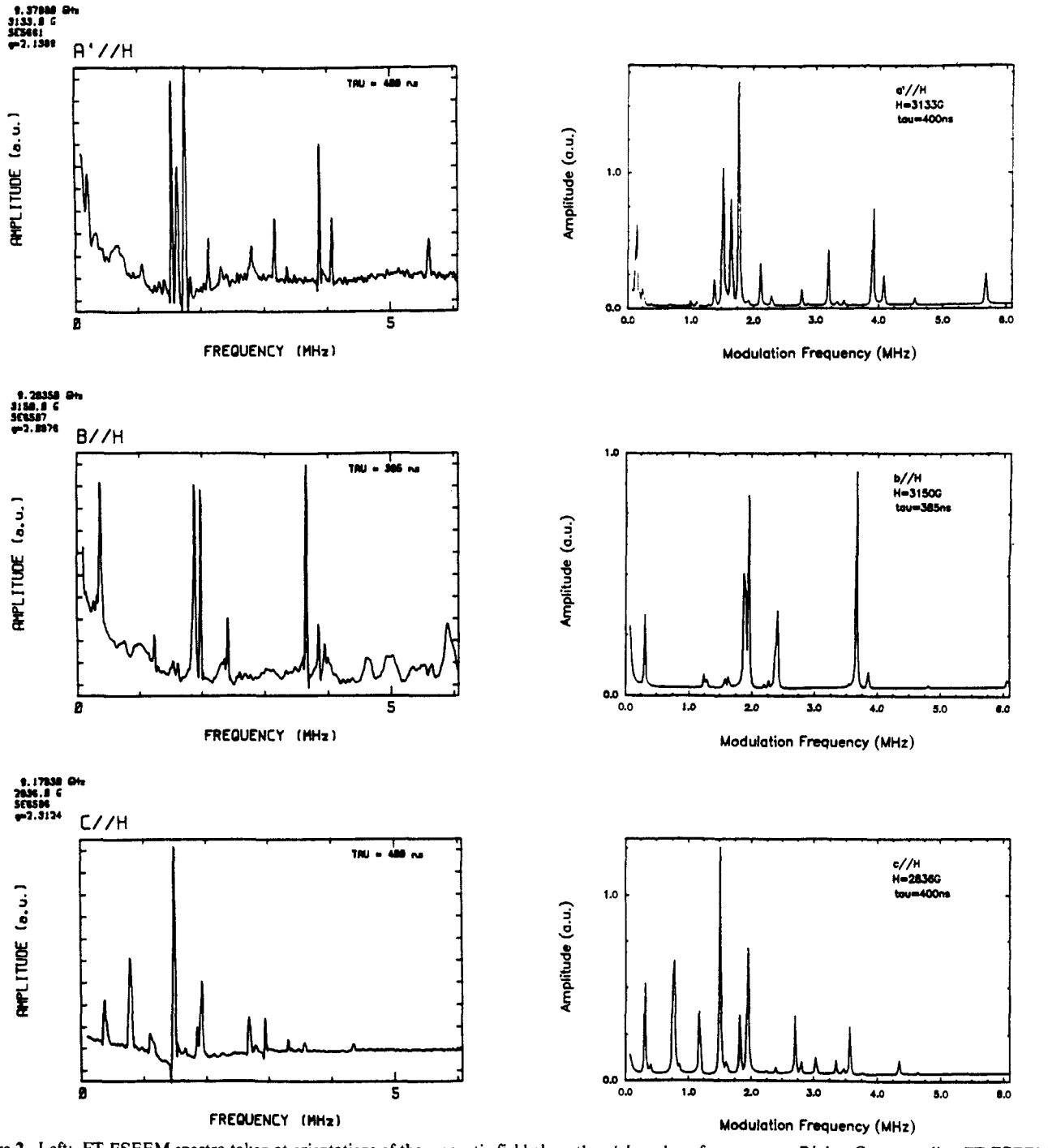

Figure 2. Left: FT-ESEEM spectra taken at orientations of the magnetic field along the *a'*, *b*, and *c* reference axes. Right: Corresponding FT-ESEEM spectra determined theoretically from the tensors listed in Table I.

The Fermi contact[16] or isotropic coupling for N1 and N4 are 1.42 and 1.37 MHz, respectively, while the total anisotropy for both nitrogens is 0.53 MHz and has a near-axial form. The corresponding hyperfine principal elements for N1 are 0.05 MHz higher than for N4, which is much greater than the largest standard deviation. However, parameter errors due to crystal mismountings are estimated to be on the order of these tensor differences and no physical meaning is therefore attached to their apparent inequalities. Maintaining the approximate 2-fold rotation relationship between the two dimethylimidazole rings in the zinc crystal structure would result in similar nitrogen coupling tensors. The derived hyperfine parameters and quadrupole interactions as discussed below are thus consistent with earlier contentions that the doped copper ion conforms to the zinc host lattice.

A correlation had been previously found between the magnitude of nitrogen isotropic coupling from N donors directly bound to Cu(II) and the amount of tetrahedral distortion of the complex, i.e., the greater the deviation from square planar, the smaller the isotropic coupling.[26] As was pointed out in this earlier study, the amount of overlap between the unpaired spin-occupied $d_{x^2-y^2}$ copper orbital and the directly coordinating nitrogen σ orbital decreases as the distortion increases and this is then reflected in a smaller nitrogen coupling.

The contention that the ligand geometry may affect the nature of spin density delocalization in a predictable manner is supported by single-crystal EPR studies on $Cu(II)Cl_4$ in planar versus tetrahedral geometries, which indicate that the ligand spin density remains essentially constant as one distorts the plane toward a tetrahedron.[27] The decrease in the amount of orbital overlap between the singly occupied copper $d_{x^2-y^2}$ orbital and the chlorine

(26) Iwaizumi, M.; Kudo, T.; Kita, S. *Inorg. Chem.* **1986**, *25*, 1546.
(27) Deeth, R. J.; Hitchman, M. A.; Lehmann, G.; Sachs, H. *Inorg. Chem.* **1984**, *23*, 1310.

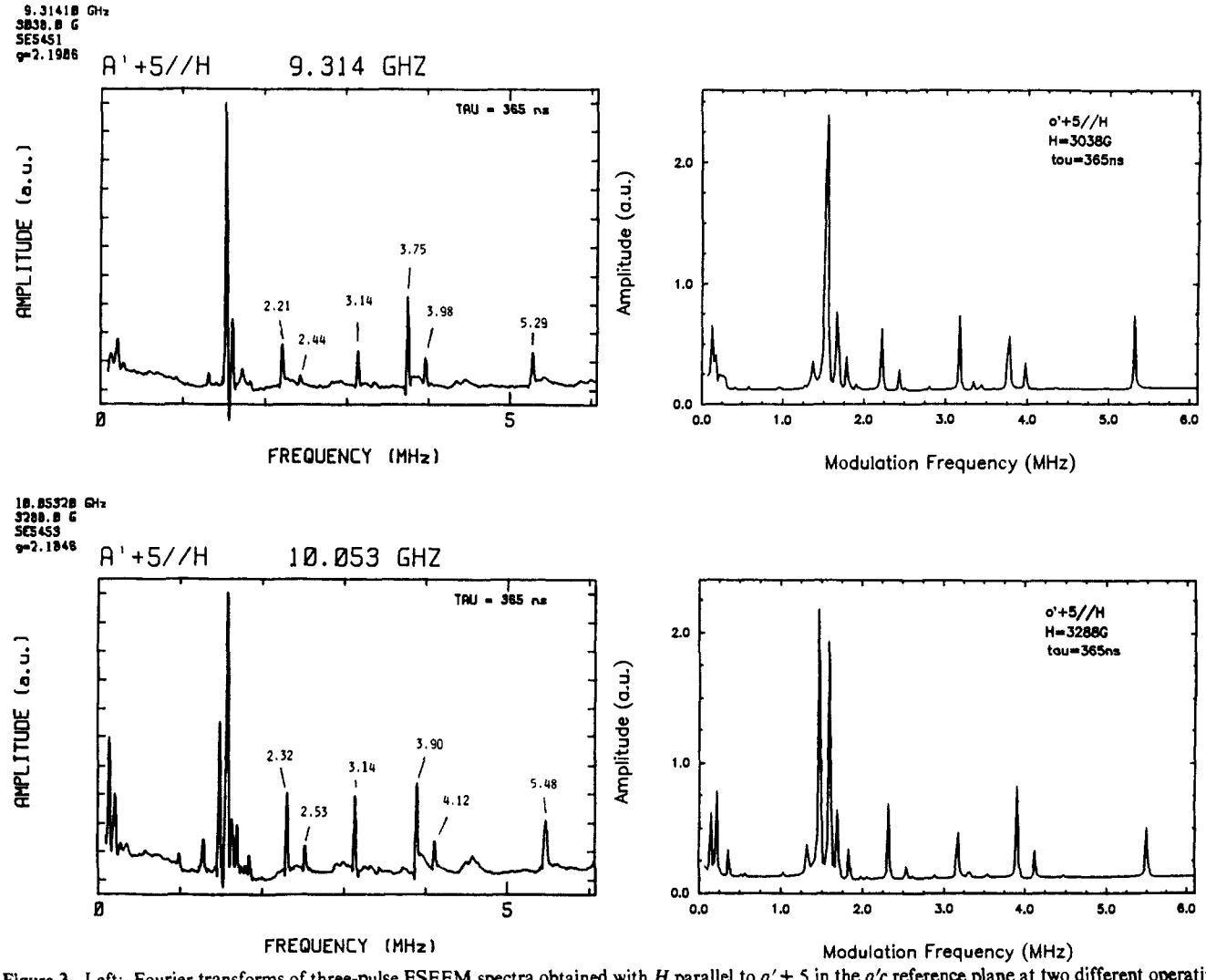

Figure 3. Left: Fourier transforms of three-pulse ESEEM spectra obtained with H parallel to $a' + 5$ in the $a'c$ reference plane at two different operating frequencies; 9.314 (top) and 10.053 GHz (bottom). The field dependencies of the labeled modulation frequencies are as described in the text. Right: Corresponding theoretical FT-ESEEM spectra, which were determined by using the tensors in Table I.

σ bond p orbital when the chlorine atoms are arranged tetrahedrally as opposed to square planar around the copper is apparently compensated by the now finite overlap between the other p orbitals of chlorine with the Cu(II) unpaired orbital. Thus, the form of the chlorine hyperfine tensor changes but the total spin density distributed onto chlorine orbitals is only slightly different for the two coordination arrangements. An analogous situation is possible for imidazole ligands in that a tetrahedral arrangement would decrease spin density in the coordinating nitrogen σ orbital, at the same time increasing delocalization either into the ring π or C–N bond orbitals. Both these hybrid orbitals have considerably less s character than the nitrogen lone-pair σ orbital, and the net result of decreased overlap between nitrogen σ and copper $d_{x^2-y^2}$ orbitals would be a decreased nitrogen isotropic coupling. However, whether the total spin density delocalized onto the ligand atoms changes as one perturbs the coordination geometry has not as yet been clearly established.

For the present system, previous single-crystal EPR studies give maximum and minimum hyperfine splittings of 23 and 17 MHz, respectively, for the directly coordinated nitrogen atoms.[9] An isotropic coupling of approximately 20 MHz can thus be roughly estimated for this tetrahedral complex. An ENDOR study of the nearly square planar complex Cu(II)(imid)$_4$ in frozen solution gave an approximate contact interaction of $\approx$40 MHz for the directly bound nitrogen.[28] Therefore, about half of the nitrogen coupling is present in the tetrahedral complex is compared to the square-planar complex, in agreement with the aforementioned trend.[26] If these results imply a reduction in total spin density delocalization onto the dimethylimidazole versus imidazole ligands in the tetrahedral as compared to the square-planar complexes, respectively, one would also expect the remote isotropic couplings to be related accordingly. The average remote nitrogen isotropic interaction of 1.40 MHz found in our study is smaller than those reported in previous ESEEM[6-8] and ENDOR[28] studies of copper-coordinated imidazole model compounds in frozen solutions, which is consistent with this hypothesis. For example, the remote nitrogen contact terms in Cu(II)(imid)$_4$[6] and in Cu(II) diethylenetriamine 2-methylimidazole[8] were determined to be 1.8 and 2.0 MHz, respectively. However, a direct comparison between these model systems may not be so easily made. Inferences on the affect of N-methylation on nitrogen hyperfine coupling come from EPR[29] and ENDOR[30] solution studies of the cation radicals of dipyridinium and *N,N'*-dimethyldipyridinium, which showed that by replacing N–H with N–CH$_3$ the Fermi contact term for ^{14}N increased from 10 to 11.7 MHz. Were this trend to be also valid for the Cu(II)–imidazole systems, the isotropic component for the remote nitrogen of the 1,2-dimethylimidazole ring would be expected to be slightly larger than for its 2-methylimidazole analogue. Thus, the apparent decrease we observe in the remote nitrogen Fermi contact in 1,2-dimethylimidazole versus the aforementioned imidazole models probably would not be due to

(28) Van Camp, H. L.; Sands, R. H.; Fee, J. A. *J. Chem. Phys.* **1981**, *75*, 1098.

(29) Johnson, C. S., Jr.; Gutowsky, H. S. *J. Chem. Soc.* **1973**, *39*, 58.
(30) Clack, D. W.; Evans, J. C.; Obaid, A. Y.; Rowlands, C. C. *Tetrahedron* **1983**, *39*, 3615.

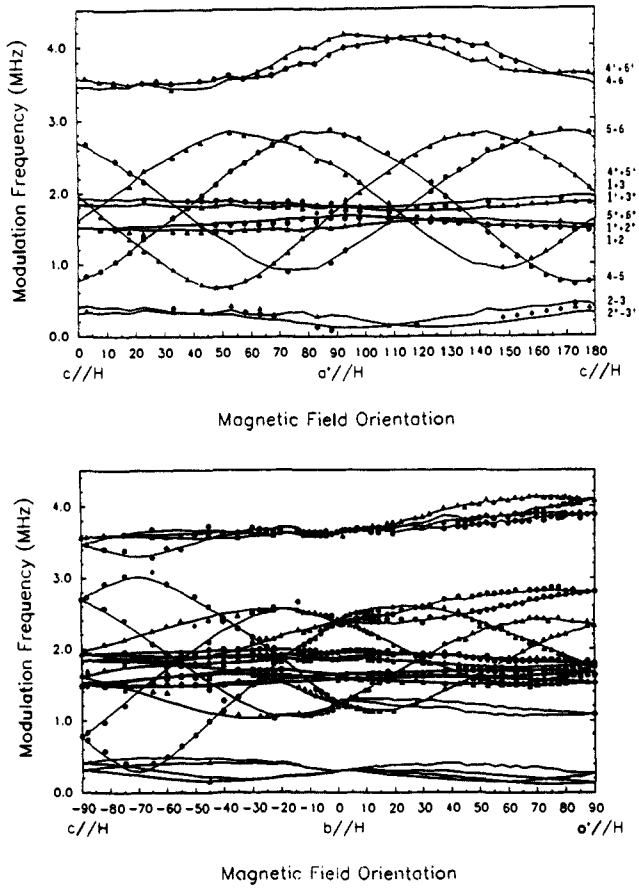

Figure 4. Angular dependencies of the primary modulation frequency lines for the two remotely coupled ^{14}N in the three reference planes. Circles and triangles refer to frequencies originating from the N4 and N1 nitrogen, respectively. Frequency line assignments, specified to the right of the upper trace, are according to the energy level scheme in Figure 5. These data were used to least-squares fit the hyperfine and quadrupole tensors of eq 1 for both nitrogens. Solid curves are calculated angular dependencies using the tensors listed in Table I and the experimental magnetic fields. The nonsmooth variation in the solid curves are due to differing spectrometer operating frequencies (and therefore resonant magnetic fields) that were employed during repetitive experiments performed in the three planes.

nitrogen methylation. However, one must also note that the frozen-solution ESEEM studies have an inherently higher uncertainty in the derived parameters due to the partial orientational averaging nature of the experiment. Nevertheless, the observed trend is consistent with the suggestion that a possible origin for an apparent decrease in isotropic coupling is the change in ligand geometry from the presumed near square planar arrangement around copper found in frozen-solution samples to the tetrahedral coordination in the present crystal system. It is clear that single-crystal ENDOR and ESEEM studies of both direct and remotely coupled nitrogens would add greatly to our understanding of the nature of unpaired electron delocalization in these and similar systems.

Anisotropic Hyperfine Coupling. The maximum hyperfine coupling does not occur along the copper–nitrogen vector but is at an angle of 40° from it. As illustrated more specifically in Figure 6, the direction of A_{max} for both nitrogens is on average 57° (56° for N1 and 58° for N4) from the normal to each imidazole plane and 38° (38° for N1 and 39° for N4) from the respective N1–C4 and N4–C5 bonds pointed away from the zinc ion. A simple multipoint model for the unpaired electron was formulated based on spin density distributed among the copper and directly coordinated ligand atomic orbitals either as listed in Table XII of Gewirth et al.[9] from SCF–Xα–SW calculations or as experimentally estimated by these same workers from the copper hyperfine and ligand superhyperfine parameters. Points representing fraction of unpaired electron were placed at crystallographically determined positions and directions either at 1 Å away from atoms in the p and d orbital lobes or at the relevant atomic positions. It was assumed that the g-tensor directions represent the reference system for the copper d orbitals. All remote nitrogen hyperfine calculations using these models gave a nearly axial tensor form but underestimated the anisotropies by 25–40% and, more critically, gave directions for the maximum hyperfine that were essentially along the copper–nitrogen vector and not less than ≈40° from the experimental values. It was concluded, therefore, that the hyperfine anisotropy must have a significant contribution from electron spin located on the imidazole ring itself. In addition, a simple multipoint electron spin model based on both copper unpaired electron character and delocalization to the directly coordinated atoms may not appropriately describe the anisotropic interaction. Evidence that spin density is located on the imidazole ring orbitals is both obviously evident from the finite remote nitrogen contact interaction and from previous ENDOR studies of Cu(II)(imid)$_4$ in frozen solution where considerable couplings to the ring protons were observed.[28] The complexity involved in the evaluation of weakly coupled nitrogen interactions with copper have been presented in two recent single-crystal ESEEM studies of Cu(II)/Ni(II) bis(tetrabutylammonium)bis(maleonitriledithiolato)[31] and Cu(II)/Ni(II) bis(*N*,*N*'-di-*n*-butyldithiocarbamate),[20] which showed that only when one-, two-, and three-center terms were also included in theoretical molecular orbital calculations of the hyperfine tensor were the observed couplings adequately explained.

Quadrupole Coupling. The quadrupole coupling tensors and their principal axes are summarized in Table I and Figure 6. The two ^{14}N tensors are equivalent within experimental certainty as expected given the nearly identical local environment of the two remote nitrogen atoms. The largest quadrupole interactions (Q_3) for both nitrogens are correlated with their respective dimethylimidazole plane normals as the corresponding directions deviate by only 1.7° and 2.3° for N1 and N4, respectively. The other two quadrupole tensor principal elements are likewise correlated (within 2.3° and 4.2° for N1 and N4, respectively) with the N–CH_3 bond (Q_1, 0.62 and 0.64 MHz) and the direction mutually perpendicular to both the plane normal and the N–CH_3 bond (Q_2). Thus, the unambiguous assignment of nitrogen quadrupole coupling parameters to an imidazole molecular geometry has been obtained for the first time in the solid state.

In order to test the reasonableness of the obtained quadrupole tensors, a simple Townes–Dailey approximation[32] using the modification for screening suggested by Gordy and Cook[33] was undertaken. Nuclear quadrupole interactions of the remote nitrogens arising from nearby point charges estimated on copper (+1.7), the directly bound dimethylimidazole nitrogens (+0.05), and the coordinated chlorines (−0.9) were calculated (using a ^{14}N nuclear quadrupole moment of 0.016*b*)[34] to be negligible (≤0.01 MHz) compared to the observed quadrupole tensor elements. The interplane N–C–N angle of 108° was close enough to 109.5° to apply directly eqs 14.120–14.122 of Gordy and Cook[33] to determine the populations of the valence nitrogen orbitals in five-membered heterocycles. We follow Gordy and Cook[33] in their assumption that the nitrogen valence orbital of the interplane C–N bond has a population of 1.25 based on the normal electronegativity difference between carbon and nitrogen (0.50). We further assume that the two C(plane)–N(remote) bond orbital populations are equivalent, both the 1,2-dimethylimidazole and in *N*-benzylimidazole. Nearly equal C–N bond lengths (1.34 and 1.37 Å) and bisection of the C–N–C angle by the N–CH_3 bond direction in the 1,2-dimethylimidazole structure[4] are consistent with this supposition. Table II lists the results of such an analysis using

(31) Reijerse, E. J.; Thiers, A. H.; Kanters, J. R.; Gribnau, M. C. M.; Keijzers, C. P. *Inorg. Chem.* **1987**, *26*, 2764.
(32) Townes, C. H.; Dailey, B. P. *J. Chem. Phys.* **1949**, *17*, 782.
(33) Gordy, W.; Cook, R. L. In *Chemical Applications of Spectroscopy Part III: Microwave Molecular Spectra*; West, W., Ed.; John Wiley and Sons: New York, 1970; Chapter 14.
(34) *Handbook of Chemistry and Physics*; Weast, R. C., Ed.; CRC Press Inc.: Cleveland, Ohio, 1974; p E-69.

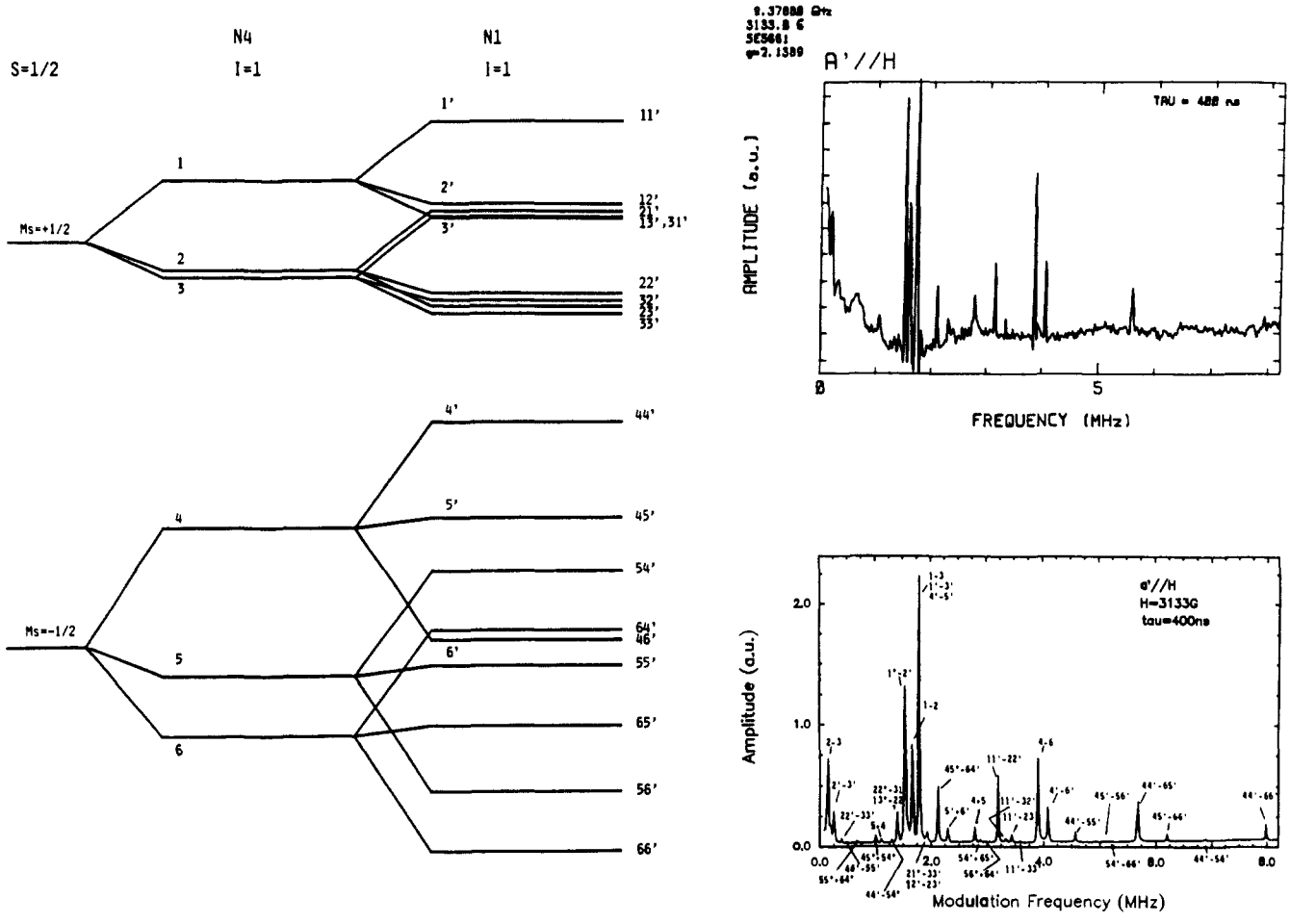

Figure 5. Left: Energy level scheme showing the interaction of the unpaired electron spin with the two $I = 1$ nitrogen nuclei calculated at $H//a'$ by using the tensors in Table I. Right: Experimental (top) and calculated (bottom) FT-ESEEM spectra at $a'//H$. Frequency lines are designated according to the energy level labels in this figure to show the origin of primary and combination modulation frequencies.

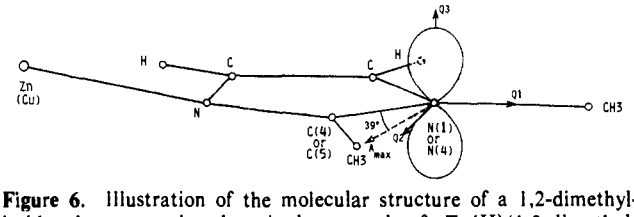

Figure 6. Illustration of the molecular structure of a 1,2-dimethylimidazole group in the single crystal of Zn(II)(1,2-dimethylimidazole)$_2$Cl$_2$ and the correspondence of the hyperfine and quadrupole tensor principal axes with the two remotely coupled nitrogens, N1 and N4.

the average e^2qQ and η from the quadrupole tensors in Table I for Cu(II)(1,2-dimethylimidazole)$_2$Cl$_2$ and published nuclear quadrupole resonance parameters for the amino nitrogen in solid *N*-benzylimidazole.[35] The nitrogen valence orbital populations for the remote and amino nitrogen as well as the net electron charges ($c-$) on these respective atoms for the two model systems are given. The N–CH_2Ph bond nitrogen orbital population (1.182) is slightly less than the corresponding population in 1,2-dimethylimidazole (1.213). Also, the net negative charge on the amino nitrogen in *N*-benzylimidazole (0.144) is less than the charge on the remote nitrogen in the copper-coordinated 1,2-dimethylimidazole complex (0.19). Although these two model systems may not be strictly comparable, the results are nevertheless consistent with the predictable, slightly higher electronegativity differences for the N–CH_2Ph versus the N–CH_3 bond. In addition, this analysis is consistent with a negative e^2qQ since the valence orbital electron occupancy found for the nitrogen p–π (1.477) is much larger than for the other two nitrogen p orbitals.

Table II. Valence Orbital Populations and Net Electronic Charge ($c-$) for the Remote Nitrogen in Cu(II) Bis(1,2-dimethylimidazole) Dichloride and the Amino Nitrogen in *N*-Benzylimidazole[a]

	1,2-dimethylimidazole	*N*-benzylimidazole
e^2qQ (MHz), η	−2.236, 0.127	−2.198, 0.232
a	1.25	1.25
b	1.213	1.182
c	1.477	1.462
$c-$	0.190	0.144

[a] Calculated according to eqs 14.120–14.122 of Gordy and Cook.[33] The *c*, *b*, and *a* populations refer to the nitrogen valence orbitals aligned along the imidazole plane normal, along the N–CH_3 (or N–CH_2Ph) bond and along the ring C–N bonds, respectively.

IV. Conclusions

The ability to accurately determine the hyperfine and quadrupole tensors of the two remote nitrogens in a coordinated 1,2-dimethylimidazole–copper complex by use of ESEEM spectroscopy has been demonstrated even when these similar nitrogens exhibit couplings near the cancellation condition.[6,10] This introduces the added complication of intense combination frequency[11,12] lines. Additionally, FT-ESEEM simulations were found to be necessary for resolving ambiguities in frequency line assignments. Multinuclear combination frequencies in the three-pulse FT-ESEEM spectra were first observed by Kosman et al.,[36] although at that time it was not known for certain if these lines were instead a consequence of detector nonlinearities. The appearance and

(35) Ashby, C. I. H.; Cheng, C. P.; Brown, T. L. *J. Am. Chem. Soc.* **1978**, *100*, 6057.

(36) Kosman, D. J.; Peisach, J.; Mims, W. B. *Biochemistry* **1980**, *19*, 1304.

subsequent assignment of combination frequencies in the present case is therefore a confirmation of the theoretical origin of such lines.

The multipoint approximation to the electron spin density has failed to describe the hyperfine anisotropy both in magnitude and in direction. A simple dipole–dipole hyperfine calculation based on multipoint electron spin models using the unpaired wave function determined previously[9] either by SCF–Xα–SW analysis or by approximate EPR parameters underestimated the observed anisotropies by 25–40% and gave angular differences in the maximum hyperfine coupling directions compared to the experimental values by about 40°. The reasons for this are unclear. However, previous analysis of such weak nitrogen couplings required the use of more elaborate molecular orbital hyperfine terms involving near-neighbor atoms to the remote nitrogens.[20,31] These results indicate that the remote nitrogen hyperfine tensor may not be such a sensitive measure of the nature of the unpaired electron wave function on the copper but are instead also reflective of the unpaired spin distributed over the imidazole ring.

The quadrupole parameters were correlated to the molecular bond directions of an imidazole nitrogen for the first time in the solid state. This tensor, rather than the hyperfine interaction, has the potential to be the key identifying factor for the origin of the magnetic coupling in ESEEM studies of more complex models or in metalloproteins. Also, the derived quadrupole parameters were found to be reasonable as compared to those found for the similar amino nitrogen in *N*-benzylimidazole.[35] The results are consistent with the slight electronegativity differences between the CH_3 and CH_2Ph groups in these two model systems. The effects of the coordinating copper and the neighboring carbon-bound methyl group in the 1,2-dimethylimidazole system apparently are either small or cancel each other to maintain this predictable trend.

Acknowledgment. We would like to thank Dr. J. Cornelius for explaining his angle selection ESEEM simulation program (NANGSEL) and Dr. J. Vitali and Dr. W. B. Mims for helpful discussions. The following grants are acknowledged: U.S.P.H.S. Grants RR-02583 and GM-40168 (to J.P.) and RRO 148601A (to H.J.S.); Grant CHE 84-17548 from the National Science Foundation (to H.J.S.).

Registry No. N_2, 7727-37-9.

Germasilene ($H_2Ge{=}SiH_2$) and Its Isomers Silylgermylene and Germylsilylene: Bond Dissociation Energies, π-Bond Energies, and Predictions of Isomeric Stability†

Roger S. Grev,*,‡ Henry F. Schaefer III,‡ and Kim M. Baines§

Contribution from the Center for Computational Quantum Chemistry, University of Georgia, Athens, Georgia 30602, and Department of Chemistry, University of Western Ontario, London, Ontario, Canada N6A 5B7. *Received March 23, 1990*

Abstract: The prototypical Ge=Si doubly bonded molecule germasilene ($H_2Ge{=}SiH_2$) and its valence isomers silylgermylene ($H_3Si{-}GeH$) and germylsilylene ($H_3Ge{-}SiH$) have been investigated in both their ground-state singlet and lowest lying triplet states. All electron ab initio quantum mechanical techniques were employed, including the effects of electron correlation via configuration interaction and coupled cluster methods. Silylgermylene is found to be the lowest lying isomer, about 6 kcal/mol below the trans-bent germasilene minimum. The π-bond energy of germasilene is predicted to be 25 kcal/mol, essentially identical with those in disilene ($H_2Si{=}SiH_2$) and digermene ($H_2Ge{=}GeH_2$). The bond dissociation energy, however, decreases in the order Si=Si > Si=Ge > Ge=Ge, and in each case is smaller than that required to break the corresponding single bonds in disilane, germylsilane, and digermane. This phenomena is rationalized by consideration of differences in first and second bond dissociation energies in the parent hydrides, Walsh's so-called divalent state stabilization energies (DSSE). Semiquantitative estimates of the relative energies of group 14 doubly bonded compounds and their corresponding divalent isomers can oftentimes be obtained by properly accounting for the DSSE.

Introduction

In the last 25 years, Si=C, Si=Si, Ge=C, and Ge=Ge doubly bonded molecules have advanced from the status of "nonexistent compounds"[1] to a class of stable molecules with a rapidly developing chemistry.[2] Conspicuous by its absence is any known example of a Ge=Si doubly bonded molecule, as either a stable compound or reactive intermediate, but it is an obvious synthetic target.

Theoretical studies of the $H_2Si{=}CH_2$,[3] $H_2Si{=}SiH_2$,[4] $H_2Ge{=}CH_2$,[5] and $H_2Ge{=}GeH_2$[6,7] multiply bonded parent compounds and their isomers are numerous as well. Attention has focused on the heavy atom–heavy atom bond distances, degree of planarity, double-bond strengths, and relative stabilities of the corresponding carbene, silylene, and germylene isomers and their barriers to interconversion. Indeed, much of what we know of

† Contribution No. 102 from the Center for Computational Quantum Chemistry.

‡ University of Georgia.

§ University of Western Ontario.

(1) Dasent, W. E. *Nonexistent Compounds*; Marcel Dekker: New York, 1965.

(2) For recent reviews of group 14 multiple bonds, see the following sources. (a) Si=C: Brook, A. G.; Baines, K. M. *Adv. Organomet. Chem.* **1986**, *25*, 1. (b) Si=Si: West, R. *Angew. Chem., Int. Ed. Engl.* **1987**, *26*, 1201. (c) Si=M (M, groups 14–16 elements): Raabe, G.; Michl, J. *Chem. Rev.* **1985**, *85*, 419. (d) M=C and M=N (M, Si and Ge): Wiberg, N. *J. Organomet. Chem.* **1984**, *273*, 141. (e) Ge=M (M, groups 14–16 elements): Barrau, J.; Escudie, J.; Satge, J. *Chem. Rev.* **1990**, *90*, 283. (f) M=M′ (groups 14 and 15 elements): Cowley, A. H.; Norman, N. C. *Prog. Inorg. Chem.* **1986**, *34*, 1. (g) Si=Si and Ge=Ge: Masamune, S. In *Silicon Chemistry*; Corey, J. Y. et al., Eds.; Wiley: New York, 1988; p 257.

(3) Schaefer, H. F. *Acc. Chem. Res.* **1982**, *15*, 283.

(4) For recent reviews of theoretical studies in silicon chemistry, see: (a) Apeloig, Y. In *The Chemistry of Organic Silicon Compounds*; Patai, S., Rappoport, Z., Eds.; Wiley: New York, 1989; p 57. (b) Gordon, M. S. In *Molecular Structure and Energetics*; Liebman, J. F., Greenberg, A., Eds.; VCH: Deerfield Beach, FL, 1986; Vol. 1, p 101.

0002-7863/90/1512-9458$02.50/0